Arabian Journal of Chemistry (2023) **16**, 104869

King Saud University

Arabian Journal of Chemistry

www.ksu.edu.sa
www.sciencedirect.com

ORIGINAL ARTICLE

Corrosion test and three-dimensional cellular machine simulation of Q235 steel by ion diffusion in different soil environments

Chunxia Xie, Jinyu An *, Zhengrong Deng, Chenglong Liu

[a] *Collage of Civil Engineering, Guizhou University, Guizhou 550025, China*
[b] *Guizhou Provincial Key Laboratory of Rock and Soil Mechanics and Engineering Safety, Guiyang 550025, China*

Received 29 November 2022; accepted 24 March 2023
Available online 30 March 2023

KEYWORDS

Metal pitting;
Corrosion test;
Unsteady diffusion model;
Cellular automata

Abstract In the actual soil environment, due to the unpredictable characteristics of metal pitting corrosion. Therefore, in this study, soil composed of different concentrations of corrosion medium was used for the mental corrosion test, and the experimental results of single ion and multiple ions were compared. At the same time, the corrosion behavior of metals is introduced in combination with the mathematical model of unsteady diffusion. In addition, the cellular automata model verification method is used to study the comparison and verification of the diffusion growth model of the model corrosion pit in different iteration steps under the discrete mathematical model. The results show that the growth and diffusion trend of corrosion pits controlled by the concentration of SO_4^{2-}, HCO_3^-, and Cl^- is consistent basically with the law reflected by cellular automata.

1. Introduction

Due to the complex, changeable, and uncertain composition of soil (Hirata et al., 2021), in recent years, soil corrosion on buried pipelines has attracted wide attention from researchers, which has seriously affected the safety of underground pipelines. Corrosion includes pitting corrosion, galvanic corrosion, uniform corrosion, intergranular corrosion, etc. (Pidaparti and Rao, 2008). However, among various corrosion types, pitting corrosion causes particularly prominent safety problems and great harm (Ezuber et al., 2020). Pitting corrosion is one of the corrosion failure modes that can cause fatigue stability of metal structures (Qi et al., 2022), and it is the root cause of corrosion failure of most bodies (Jahns et al., 2014). Pitting pits develop randomly, and most of them occur at any position on the free surface (Wang, 2021). Pitting corrosion is difficult to be recognized by the naked eye due to its micro-scope and limitation. To further understand pitting, confocal laser scanning microscopy (CLSM) (Wei et al., 2020) and scanning electron microscopy (SEM) (Chen et al., 2021) were used to obtain more information about the pitting pits. However, the growth of pits is an extremely complex process, which is affected by the differences of metal material composition (Chen et al., 2008), physical and chemical inhomogeneity (Rybalka et al., 2010), physical and chemical properties of corrosive media (Stępień and Stafiej, 2018) (temperature, -PH, water content, bicarbonate, chloride ions, electrical conductivity) and other factors. Key features such as corrosion rate, pit size, and pit morphology will also be different (Chung et al., 2021). Pitting corrosion is a kind of chemical reaction with corrosion kinetics characteristics. At the same time, there is a crystalline passivation film on the metal surface (Xuefeng et al., 2021), but due to the different roughness of the metal surface, the severity of pitting corrosion is also different (Zenkri et al., 2022). When pitting occurs, a de-passivation reaction

* Corresponding author.
E-mail address: 450044789@qq.com (J. An).

https://doi.org/10.1016/j.arabjc.2023.104869

occurs on the metal surface (Saunier et al., 2006), and the protective effect of a surface crystalline passivation film on the substrate decreases (Wang et al., 2021), and the passivation film becomes active. When the local acidity is changed, the passivated film reacts with the acid ions and dissolves, and the anodic reaction with autocatalysis occurs in the local location, which accelerates the corrosion rate (Apostolopoulos et al., 2013). The cathode reaction that alkalizes the environment occurs outside the corrosion pit (Pérez-Brokate et al., 2017), leading to the formation of micro-galvanic corrosion cells, which are accompanied by the characteristics of a large cathode and small anode (Long et al., 2020).

Theoretical models of mathematical probability are widely used to describe the growth and evolution process of corrosion pits, including the lognormal distribution method, simple statistical method, time series method of random corrosion events, uniform (non-uniform) Poisson distribution, and Fick's law. Researchers generally focus on three aspects corrosion rate, depth of corrosion pits, number of corrosion pits, and the connection between mathematical theoretical models (Apostolopoulos et al., 2013). Liu et al. (Liu et al., 2020) obtained that the corrosion rate of pipeline steel in the soil of different thicknesses was no more than 0.05 mm/y by using the weightlessness test and electrochemical measurement.

Feng et al. (Feng, 2020) found that the corrosion pit depth of steel is linear with the ultimate strength of the material. Cui, Ma et al. (Cui et al., 2019) established a mathematical model to describe the growth of pits and found that the growth follows non-uniform Poisson distribution and logarithmic Gaussian distribution. Xu et al. (Xu et al., 2022) concluded from the experimental results that the initial pervasion of the pit was majorly centralized in the depth direction, and it was very likely to form a through the pit. The evolution of corrosion is a beyond-measure complex corrosion kinetic process (Valor et al., 2007). Pérez-Brokate et al. (Pérez-Brokate et al., 2016) found that the corrosion rate is directly controlled by the probability of an anode or cathode reaction. Acidity has an autocatalytic effect on metal corrosion. The corrosion rate in the acidic region is high, meanwhile, the metal is smooth. However, in addition to the research contents and technique methods proposed by the above researchers, the influence of the diffusion of corrosive ions in the external soil on the corrosion of metal pipelines is also of great significance for the study of structural stability. Therefore, this paper will propose a mathematical model of corrosion diffusion.

Numerical simulation has gradually become one of the most significant methods for model reproduction (Chang et al., 2022). As early as 1940, von Neumann proposed the concept of cellular automata. Cellular automata (CA) are used on a microscopic or mesoscopic scale (Saunier et al., 2006) to model the corrosion growth process of the metal matrix into a discrete mathematical model (Wang and Han, 2015), which is transformed into a model with complex function properties through simple transition function rules (di Caprio et al., 2016). Cellular automata have been widely used in many scientific fields to solve different problems (Zhang et al., 2012). Zhang et al. (Bartosik et al., 2014) compared the numerical results with the model results to establish a three-dimensional CA model for the dendrite growth of multi-component alloys. Bartosik, L et al. (Wang et al., 2019) found through research that the anode and cathode on the spatial separation effect were related to the pH of the electrolyte on the growth and forming time of corrosion pits. Wang et al. (Rusyn, 2015) adopted a simple three-dimensional CA model and obtained the rule of corrosion layer growth and chromium element migration through the correlation between simulation results and experimental results. B.p.royn et al. (Bhandari et al., 2015) developed a new transition rule for conversion to verify the consistency of the actual situation with the pitting of alloys in CA -simulated acidic or alkaline solutions. Some researchers have taken the initiation and development of pits into consideration in the establishment of CA models (Fatoba Olusegun,and Akid Robert, 2022). However, the location and size of the pits on the metal matrix play an important role in the subsequent study of structural stability (Zhou, , prepublish(2022).).

In this study, a mathematical model of the influence of corrosive ion diffusion on the size of the pitting was proposed in connection with the theoretical model of diffusion, and the change of surface corrosion process of Q235 steel under a real soil environment was studied. The corresponding transformation rules were set according to the sample concentrations of chloride ions, sulfate ions, and bicarbonate in different soil environments, and the appropriate three-dimensional CA model was established to observe the corrosion evolution process of the metal matrix surface, and finally, the correlation between the three-dimensional CA simulation and the test results was verified.

2. Experiment

2.1. Soil

The corrosion behavior of buried steel pipelines in the soil is affected by the environment and various physical and chemical factors of soil (Wang Xuankai, et al., 2022), including sulfate ions, bicarbonate ions, chloride ions, water content, -pH, conductivity, etc. Considering the difference between actual soil and simulated soil solution on the growth of pipeline corrosion pit (Liu Menglei, et al., 2022). In order to better explore the pipeline corrosion, the experiment adopts actual soil to simulate the external environment of metal, and appropriately changes the concentration of corrosive ions in natural soil, so as to form a better external environment for the pipeline. The soil was taken from Guiyang, Guizhou Province, and its surrounding areas, and the main soil composition was Guizhou's special red clay. The preparation process of the experiment is divided into three steps:

(1) The soil is fully dried, then ground into smaller particles, and then sifted with a 2 mm sieve.
(2) Take the soil after screening and extract the soil extract, and determine the content of ions in the soil according to the Experimental Method of Soil Chemistry.
(3) According to the requirements of the experimental scheme, combined with the final results of the determination of the soil ratio.

By changing the concentration of typical ions, it is known that different soil components will have a great influence on the corrosion behavior of metal pipes. n this study, three soil matching methods are used to compare the metal corrosion under the action of high concentration Cl- alone ([40]), the action of Cl^- with SO_4^{2-}, and the synergic action of Cl^-, HCO_3^- with SO_4^{2-} (Li Xiaohan, et al, 2021). The ratio scheme of soil ion concentration is shown in Table 1. And soil blending map is shown in Fig. 1.

2.2. Materials

Because Q235 steel is homogeneous low-carbon steel, the comprehensive performance is better. It is often used as building steel, usually as the main material for structural buildings, cars, machines, and bridges. The characteristics of carbon steel determine that it has stronger corrosion resistance under harsh external conditions. Especially in red soil, various acid and alkali ions contained in red soil will play a role in the infiltration and erosion of Q235 steel (Safira Fitri, et al., 2018), damage the surface of steel and seriously affect its structural stability (Cai Shuo, 2022).

Table 1 Soil physicochemical factors composition ratio scheme table.

Matching ratio scheme	Cl^-(mol/kg)	HCO_3^-(mol/kg)	SO_4^{2-}(mol/kg)	Content of water%	-pH
1	2.54	0	3.16	25	3.0
2	4.24	0.192	0.08	25	9.0
3	4.83	0	0	25	4.9

Fig. 1 Soil treatment and allocation.

Table 2 Tempering chemical composition of Q235 (%).

composition	C	Si	Mn	P	S
Percentage	≤0.22	≤0.35	≤1.40	≤0.045	≤0.05

In addition, considering that the ultimate goal of this study is to study the leakage and diffusion law of natural gas-buried steel pipes, Q235 steel is currently used in large-scale medium-pressure and above-pressure pipe networks in Guizhou. in the interest of corroding the actual working conditions, the sake of providing more valuable experimental data for subsequent research, and better combining the experiment with the actual project, the experimental material to be used in this study is Q235 steel, and its chemical composition is shown in Table 2. The length, diameter, and thickness of the steel tube sample are 5 cm * 1 cm * 1 mm, as shown in Fig. 2. After that, the sample was placed in ethylene glycol, ultrasonically cleaned for 30 min to remove the surface grease, and then the residual impurities were cleared with distilled water, placed in a drying oven to dry the water and put into a sealed bag for use.

Take three lengths, widths, and height specifications for a 33 cm*33 cm*5cm laboratory special corrosion prevention tray. According to the above ratio scheme, the experimental soil and Q235 steel are put into the tray and numbered, as shown in Fig. 3. Because the temperature change range of the soil in the real external environment is not large (Changxu Huang, et al., 2021), the temperature is an important environmental invariant that needs to be strictly controlled. Therefore, the equipment used in the experiment is an electrothermal constant temperature test chamber to cultivate the soil. The experimental temperature is set to 30 °C (Qi Gang, et al., 2022). During the test, the selected Q235 metal material is subjected to metal electrochemical measurement (Bianli, 2021); including open circuit potential measurement, potentiodynamic measurement, and electrochemical impedance measurement. The measurement period is 7d, 14d, 21d, and 30d to study the change in metal corrosion rate.

Fig. 2 Sample size measurement diagram.

2.3. Electrochemical analysis

Corrosion between metals is a common natural phenomenon, which not only causes serious waste of resources in all walks of life, hinders economic growth, but also easily leads to greater

Fig. 3 Soil buried pipe setting.

safety hazards in the industrial production process (Lan Yujie, et al., 2021). The main methods of corrosion research include surface analysis techniques based on X-ray diffraction, metallographic microscope, and scanning electron microscope analysis. The weight loss method, salt spray test method, and electrochemical analysis technology of corrosion rate were studied (Puspalata, 2022). Electrochemical testing technology is widely used in the study of corrosion science because of its simple operation (Miao, 1334), short measurement time, small damage to materials, accurate measurement results, and comprehensive information on electrode corrosion kinetics (Li, 1985). The electrochemical measurement methods used in this study include:

1. Open circuit potential measurement: In this study, the metal was buried in a tray with soil as the corrosive medium, and the electrochemical measurement circuit was connected. Corrosion and passivation of metals or alloys can be studied by measuring the open circuit potential, which does not cause polarization and is also beneficial to protect materials.
2. Potentiodynamic measurement method: through the polarization curve analysis of metal and alloy corrosion resistance, metal dissolution and passivation process is a widely used electrochemical test method, mainly including polarization curve method and cyclic voltammetry method, by the steady-state polarization curve position and shape characteristics can analyze the electrochemical behavior characteristics of the corrosion process, can calculate some important corrosion behavior parameters, analyze the corrosion process, judge the corrosion resistance.
3. Electrochemical impedance method: Electrochemical impedance technology has developed rapidly in recent years, and its application range has also expanded from the traditional electrochemical field to many fields such as chemical power supply, biofilm performance, conductive materials, and material surface modification. Electrochemical impedance technology also has important applications in the field of corrosion. It can be used to study the changes in electrode surface during corrosion and the damage of corrosive substances to coatings and coatings, as well as metals.

In this study, the metal was electrochemically measured in the electrochemical workstation of the three-electrode system. The metal platinum sheet was used as the auxiliary electrode, the sample in the soil was used as the working electrode, and the saturated copper sulfate electrode was used as the reference electrode. Before measuring the AC impedance, the potential polarization range of the open circuit potential is set to −2.5 V to + 2.5 V, the current range is 2 mA, the power frequency is 50 Hz, and the open circuit potential measurement time is set to 1800 s, until the current is stable, the AC impedance frequency is $1.0 \times (10^5 \sim 10^{-2})$ Hz.

2.3.1. Curve of polarization

Fig. 4 shows the polarization curves of Q235 steel under actual experimental soil at different concentrations of Cl^-, HCO_3^- and SO_4^{2-} as well as different -pH. it can be seen that under the condition of slightly changing the concentration of Cl^-, SO_4^{2-} and -pH value, and controlling the water content unchanged, the cathodic polarization curve in scheme 1 has reached the limiting current density value of O_2 reduction at-0.27 V, and the cathodic polarization curve in scheme 3 has reached the limiting current density value of O_2 reduction at-0.75 V. It can be seen from this that the polarization curves of scheme 1 and scheme 3 have obvious deviation, the corrosion current density increases, the polarization curve has small fluctuation, the changing trend has changed, but there is no obvious activation-passivation zone in both schemes. It can be clearly seen that the self-corrosion potential E_{corr} of scheme 1 is greater than that of scheme 3, indicating that the former may have a lower corrosion tendency than the latter. However, according to the soil ratio scheme, the -pH of scheme 1 is 3.0, while the -pH of scheme 3 is 4.9. Under strongly acidic conditions, the corrosion of metal has an autocatalytic effect, which may lead to the corrosion rate of scheme 1 being slightly larger than that of scheme 3. For scheme 2, HCO_3^-, which will passivate the metal, is added, and the -pH is set to an alkaline condition. It can be seen from the polarization curve that the E_{corr} of scheme 2 is larger than that of scheme 3. The reason may be that the added HCO_3^- forms a passivation film on the metal surface during the corrosion reaction, thus reducing the rate of corrosion reaction.

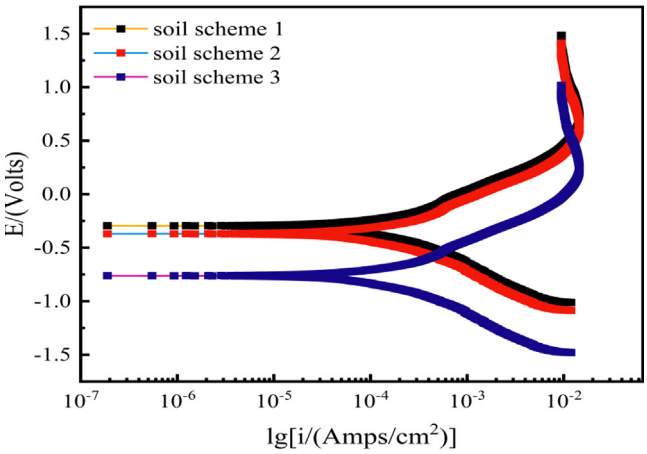

Fig. 4 Polarization curves obtained by electrochemical measurement of three ratio schemes in actual soil.

Combined with the Tafel formula, the polarization curves of the three schemes are fitted. The fitted data results and corrosion rates are shown in Table 3. In scheme 1, $\beta_c > \beta_a$, indicating that the corrosion reaction rate is controlled by the cathodic reduction reaction. In schemes 2 and 3, $\beta_c < \beta_a$, indicating that the corrosion rate in these two schemes is controlled by the activation dissolution reaction of the anode. According to the corrosion rate of Q235 steel in three different soil environments, it can be seen that schemes 1 and 2 conform to the basic law. However, the soil of scheme 3 contains neither SO_4^{2-} nor HCO_3^-, which promotes the corrosion of metals. The reason why the slowest rate may be that only a single variable Cl^- is added. In the presence of only one factor, the effect on metal corrosion rate is lower than that of multiple corrosion.

2.3.2. Electrochemical impedance spectroscopy

The soil of the three experimental schemes was electrochemically measured on the 7th, 14th, 21st, and 30th days, respectively, as shown in Fig. 5. According to the Nyquist diagram obtained from the electrochemical measurement on the 7th day, it can be observed that soil scheme 3 represents the addition of high concentration Cl^- alone in the soil corrosive medium. Its Nyquist diagram is composed of an incomplete capacitive arc. The reason may be that there is a very small amount or no SO_4^{2-} and HCO_3^- in the soil environment with high Cl^- content and as the main influencing variable. In the early stage of the corrosion reaction, the high concentration of Cl^- in the soil reacts with Fe on the surface of Q235 steel to produce Fe^{2+}, and Fe^{2+} further hydrolyzes under the action of electrode polarization to form a dense oxide film containing Fe_3O_4. This oxide film protects the metal and prevents the corrosion reaction, resulting in an incomplete capacitive arc curve.

However, in the data measured on the next 14d, 21d, and 30d, the capacitive reactance arc radius on the Nyquist diagram of the soil ratio scheme 3 shows a gradual increase from the low-frequency region to the high-frequency region at three times. The result may be due to the hydrolysis reaction of Cl^- and Fe in the early stage, resulting in a layer of passivation film attached to the surface, and the size of the capacitive reactance arc is proportional to the corrosion resistance of the metal. With the increase of the capacitive reactance arc, the corrosion resistance of metal increases gradually, and the corrosion reaction rate becomes slower and slower.

For the soil ratio scheme 1, it is controlled by Cl^- and SO_4^{2-} with higher concentrations. From the Nyquist diagram, it is observed that there is a less obvious Weber impedance phenomenon on the 7th day, and the Weber impedance phenomenon disappears on the 14th day. At the same time, the radius of the capacitive arc gradually increases, and the radius does not appear to continue to increase until the 21st day. During this period, the corrosion rate of the metal showed a decreasing trend. However, on the 30th day, the radius of the capacitive arc on the Nyquist diagram suddenly decreases, which indicates that the corrosion rate of the metal shows an accelerated trend. The reason for this situation may be due to the high concentration of SO_4^{2-} in the soil ratio scheme. In the later stage of the corrosion reaction, due to the high ion concentration, the oxide film formed on the metal surface is destroyed, resulting in the accelerated corrosion rate of the metal.

In the SO_4^{2-}, HCO_3^-, and Cl^- three are high concentrations of soil ratio scheme 2, the corrosion rate of the metal is affected by the combined effect of three ions. On the Nyquist diagram, it can be observed that there is a clear Weber impedance line segment phenomenon on the 7th and 14th days, which indicates that there is a large difference between the concentration of corrosive ions on the electrode surface and the concentration of soil reactants in the soil. Due to the concentration difference, there will be a process of reactant diffusion from the soil body to the electrode surface in the soil. This diffusion process is usually shown on the electrochemical impedance spectroscopy (EIS). Similarly, if the electrode reaction rate is too high, the electrode reactant will also diffuse from the solution layer close to the electrode surface to the soil body. The reason may be that the concentration of corrosive ions in the soil is much higher than that of the electrode and the metal surface, which leads to the diffusion of corrosive ions from the soil to the electrode and the metal surface. At the same time, from the data observation results of the 7d, 14d, 21d until the 30d, the radius of the capacitive arc of the ratio 2 shows an increasing trend in the three measurement times until the disappearance of the Weber impedance line segment phenomenon, and the line segment on the graph cannot become a complete capacitive arc. This phenomenon shows that the corrosion rate of the metal in this kind of soil ratio is getting slower and slower.

According to the three schemes of soil ratio, through the results of this experimental study, it can be observed that under the same conditions, in the case of scheme 3, only Cl^- as a single variable to control soil corrosion behavior, the corrosion rate of metal will be due to Cl^- concentration is too high and generate oxide film to inhibit the corrosion rate of the metal. For the soil ratio scheme 1, which is controlled by the high concentration of Cl^- and SO_4^{2-} as the influencing factors, the high concentration of SO_4^{2-} exists in the soil and reacts with the passivation film on the metal surface, which destroys the surface structure formed by the reaction with Cl^- in the early stage of metal corrosion, resulting in the corrosion rate of the metal decreasing first and then increasing. At the same time, for the soil ratio scheme 2 controlled by high concentrations of SO_4^{2-}, HCO_3^-, and Cl^-, the Nyquist diagram shows a more obvious Weber impedance phenomenon, and the metal corrosion rate under the combined action of these three ions also shows a gradually decreasing trend.

Table 3 Results of the polarization curve fitting data of Taffel slope.

Soil Scheme	β_a(mv)	β_c(mv)	J_{corr}(A·cm^2)	E_{corr}(V/m)	Corrosion rate(mm/a)
1	196.53	269.23	7.2805×10^{-5}	−0.29433	0.85087
2	558.14	197.32	7.6606×10^{-5}	−0.56230	0.89531
3	572.12	386.53	4.5693×10^{-5}	−0.76346	0.53403

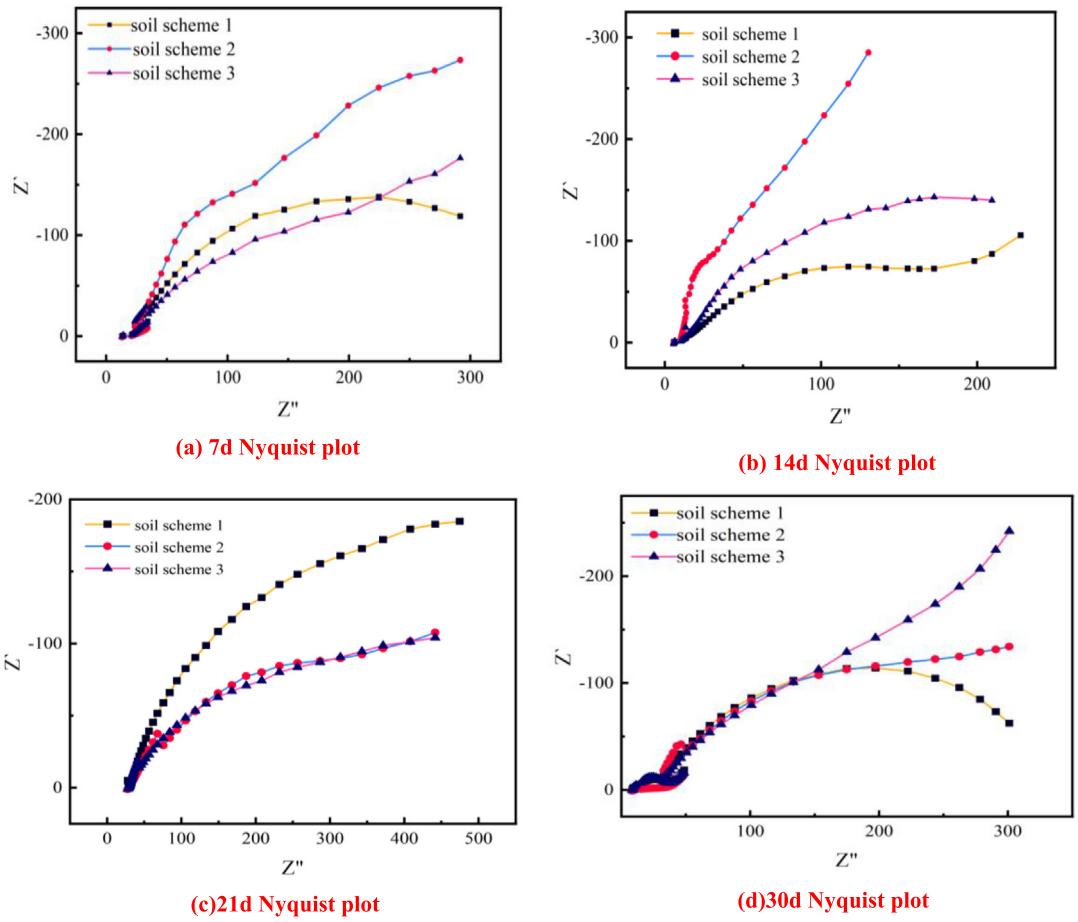

Fig. 5 Nyquist plots of electrochemical measurements of Q235 steel in three soil ratio schemes.

2.4. Theoretical model verification

Most researchers focus on the results of ion corrosion of metal pipes. At the same time, the buried environment of metal plays an important role in the corrosion process of metal. Starting from the soil particle size, water content, total salt content and -pH, etc., due to the inhomogeneity between various physical and chemical components in the soil, as well as the electrification of the soil system itself and the different distribution concentrations of ions in the soil, the diffusion of corrosive ions in the soil is affected by the concentration and soil potential gradient. Therefore, in this case, Fick's law cannot be directly used to describe the diffusion process of ions in the soil system. However, based on the thermodynamic point of view and the basic kinetic principle of the material diffusion process, and then based on Fick's first and second laws as the basic theory of formula extension, a hypothesis is made on the influence of corrosive ions in soil on the corrosion of metal pipeline surface.

2.4.1. Diffusion equation (11)

To Fick's second law as the foundation, the diffusion of ions in the soil is considered as an unsteady state diffusion process of change over time, the ion concentration in the soil is expressed as a function of time c (x, t), at the same time, the free energy of the ion is expressed as time function u (x, t), at the same time, concentration and free energy between the closely linked, The relationship between them can be expressed as follows (Law, 1985):

$$c(x,t) = e^{\frac{u(x,t)-u_0}{RT}} \tag{1}$$

Substituting (1) into Fick's first law gives a representation of the free energy of ions:

$$j = -D\nabla\left[e^{\frac{u(x,t)-u_0}{RT}}\right] \tag{2}$$

Where j is the number of ions passing through a unit volume within a unit of time, referred to as flux; D is the diffusion coefficient of corrosive ions. In addition, because the soil is an uneven system; when the free energy of ions in the soil is represented at time points, it is not only affected by the concentration of ions; but also by the action of the excess electric potential θ(x,t) generated by the external electric field in the soil system. Therefore, Fick's law was connected to the Nernst-plank equation, and in the presence of both ion concentration gradient and electric field gradient, the free energy of corrosive ions was expressed as (Hang and Jiahua, 1998):

$$\Phi(x,t) = x(x,t) + \theta(x,t) \tag{3}$$

Therefore, the relationship between concentration and free energy in the soil external electric field can be expressed as:

$$\Psi(x,t) = e^{\frac{\phi(x,t)-u_0}{RT}} \tag{4}$$

Among them, the Ψ (x, t) represent the ion concentration of coordinates ×, t represents the time, u 0 means ion standard free energy, R for the gas constant, and it is the absolute temperature. Based on the above derivation, the model of corrosive ion diffusion in the soil can be expressed by formula (5)–(21) (Lei et al., 2009). By substituting (2) into Fick's first law and second law, the unsteady diffusion equation of ions in the soil can be written as:

$$\mathrm{J} = -\nabla\ \psi(\mathrm{x},\mathrm{t}) \tag{5}$$

$$\frac{\partial\Psi(x,t)}{\partial t} = \nabla\cdot[D\nabla\Psi(x,t)] \tag{6}$$

Considering the shape of the metal material selected in this experiment, the soil at the distance h from the circular metal pipe is taken as the origin of coordinates (the interface of x = 0), and the diffusion type is assumed to be unsteady diffusion. Within the thickness of h (the thickness of h is very small) is an ideal state where corrosive ions do not exist and the shape is a ring cylinder. And the electric potential at the origin of that coordinate is close to zero. Suppose ion within unit time within the thickness of the metal pipe migration an average speed of v, in unit time through the loop number of ions on the surface of the cylinder as follows:

$$\frac{\mathrm{dN}}{\mathrm{dt}} = S\cdot\tilde{\mathrm{N}}\mu\cdot c(x,t) \tag{7}$$

N is the number of ions and S is the surface area of the ring cylinder.

Then (2) can be written as:

$$\frac{\mathrm{dN}}{V\mathrm{dt}} = -\frac{\mathrm{D}}{RT}c(x,t)\nabla u(x,t) \tag{8}$$

According to (3), (7), and (8), the motion velocity of corrosive ions in the soil is:

$$\tilde{\mathrm{N}}\mu = -\tfrac{\mathrm{D}}{RT}\nabla\Phi(\mathrm{x},\mathrm{t}) \tag{9}$$

According to (4), the expression of flux j can be divided into:

$$j = -De^{-\frac{\theta(x,t)}{RT}}\cdot\nabla\Psi(x,t) \tag{10}$$

However, corrosive ion concentration in the soil at different positions is different, so in the application of ion concentration shall adopt the average concentration in the space system, so the Ψ (x, t) and $e^{\frac{-\theta(\mathrm{x},\mathrm{t})}{RT}}$ should is the average per unit time, in the assumption of ideal annular space, research by annular surface to the number of ions, Therefore, the flux equation of diffusion can be expressed as:

$$j = -\frac{D}{V}\int_0^V e^{\frac{-\theta(x,t)}{RT}}dV\cdot\nabla\Psi(x,t) \tag{11}$$

2.4.2. Diffusion model

Considering that temperature plays an important role in the diffusion coefficient D, the higher the temperature, the faster the ion diffusion, and the greater the diffusion coefficient D. Therefore, when studying the diffusion model of ions in the soil, the temperature is used as a constant invariant, combined with the material length of 5 cm and diameter of 1 mm selected in the experiment, the surface area of the ideal ring cylinder is 100π (1 + h), and the concentration of corrosive ions is c0. Since chloride ion is a single important variable and plays a major role in corrosion in the corrosive environment of soil ratio 3, the chloride ion concentration of scheme 3 of soil ratio is taken as an example, and c_0 = 4.83 mol / kg. At the same time, the electric field is assumed to be independent of the time at the soil interface of the coordinate origin. The number of ions passing through the ring cylinder in unit time is:

$$\frac{\mathrm{dN}}{\mathrm{dt}} = 100\pi(1+h)\cdot\mathrm{v}\cdot c(x,t) \tag{12}$$

From (7) and (11), the flux equation at x = 0 is.

$$\frac{dN}{Vdt} = j = -\frac{D}{h}\int_0^h e^{\frac{-\theta(x,t)}{RT}}dx\cdot\frac{\partial\Psi(x,t)}{\partial x}\mid x=0 \tag{13}$$

According to (6) and the assumed conditions, four definite solution conditions for the boundary of unsteady diffusion are determined:

$$\frac{\partial\Psi(x,t)}{\partial t} = D\frac{\partial^2\Psi(x,t)}{\partial x^2} \tag{14}$$

$$\Psi(0,t) = \Psi_0 = c_0 = 4.83mol/kg \tag{15}$$

$$\Psi(h,t) = 0 \tag{16}$$

$$\Psi(h,t) = f(t)\neq 0 \tag{17}$$

Ψ in the definite condition is zero in Ψ value of × = 0 interface Ψ (h, t) = f (t) refers to the soil and metal distance as h, diffusion equation and the basic relationship between the change of time. Here, four particular solution conditions are used to obtain:

$$\Psi(x,t) = 4.83\left\{1-\sum_{n=0}^{\infty}\frac{4}{(2n+1)\pi}e^{\left[-\frac{D\pi^2}{4h^2}(2n+1)^2t\right]}\cdot sin\left[\frac{x}{h}(2n+1)\frac{\pi}{2}\right]\right\} \tag{18}$$

Where n = 0,1, 2, ….

Substitute (4) into (18):

$$c(x,t) = 4.83e^{\frac{-\theta(x,t)}{RT}}\left\{1-\sum_{n=0}^{\infty}\frac{8}{(2n+1)\pi}e^{\left[-\frac{D\pi^2}{4h^2}(2n+1)^2t\right]}\cdot sin\left[\frac{x}{h}(2n+1)\frac{\pi}{2}\right]\right\} \tag{19}$$

In summary, the dynamic distribution equation of chloride ions in soil can be obtained by connecting (18) and (13):

$$N = 4.83\times 100\pi(1+h)\times\int_0^h e^{\frac{-\theta(x,t)}{RT}}dx\left[1-\sum_{n=0}^{\infty}\frac{8}{(2n+1)\pi^2}e^{\left[-\frac{D\pi^2}{4h^2}(2n+1)^2t\right]}\right] \tag{20}$$

Thus, the total amount of ions diffused into the soil at equilibrium is:

$$N_\infty = 4.83\times 100\pi(1+h)\int_0^h e^{\frac{-\theta(\mathrm{x},\mathrm{t})}{RT}}dx \tag{21}$$

Do to (20) and (21) ln (1-N/N_∞) of time t composing chart shown in Fig. 6.

Taking t = 300 as an example, from equation (20), we can observe the changes of ions with time by referring to the terms of the equation when n = 0. It is concluded that (1-N/N_∞) in the convergence speed when t > 0. This is consistent with the

results obtained by electrochemical measurement in soil proportion-scheme 3.

3. Corrosion three-dimensional cellular modeling

The results of the experimental data have a crucial impact on the construction of our model. According to the test results, for the three soil ratio schemes, the corrosion rate of the metal is very different under different ion concentrations and the number of ions. A series of research problems such as the corrosion behavior of soil to metal is considered as the diffusion of ions in the soil. In addition, in the early stage of corrosion behavior, considering that the metal will undergo local pitting corrosion due to the influence of the soil environment, this study considers that pitting corrosion occurs on the surface of metal materials within 30 days, forming corresponding pitting pits. Therefore, this study uses a three-dimensional cellular machine combined with the content of each ion in the soil to model the growth and diffusion of pitting pits in the initial stage; and observe and restore their characteristics.

In addition, according to our experimental soil ratio, the concentration range is mainly selected based on the existing research results of pitting corrosion. The main purpose is to speed up the pitting corrosion rate and produce pitting perforation as soon as possible. Therefore, our experiment is the same as the three-dimensional cell machine simulation pitting corrosion.

3.1. Cellular automata

By considering the behavior of imitating the human brain and processing in the framework of complete discretization, and each cell has its own internal state and is composed of a limited amount of information, von Neumann proposed the concept that cellular automata (CA) is a discrete dynamic model in time, space and state (Wang and Han, 2016). Cellular automata (CA) is composed of cellular, cellular space, cellular neighbors, evolution rules (transition function), cellular state, and time. At the same time, in the case of a series of simple rules, the CA model is also a general term for a class of models or a framework of methods (Guiso et al., 2022).

Cells are the most basic components and units (also known as primitives) existing in cellular automata, which are distributed on the lattice points constructed by one-dimensional, two-dimensional, or multi-dimensional Euclidean space, and can constantly update the states at different time points according to the transformation rules (Fatoba et al., 2018). The set of points distributed in space is called cellular space, and two-dimensional cellular space is widely used in research. Theoretical research shows that cellular space can be infinitely extended in all dimensions (Chen et al., 2015), but this ideal condition cannot be achieved in practical research simulation. In order to find the closest method to infinite space, researchers have proposed the concept of periodic boundaries. The so-called periodic boundary refers to the topological torus formed by the upper and lower left and right respectively. The simple top-level periodic boundary conditions are connected as shown in Fig. 7.

Cellular and cellular space only belong to the static components of the cellular automata (CA) system. In order to represent the model in a dynamic way, it is necessary to define a neighbor cell that can complete the transformation rules within the spatial range: that is, the cellular state at the next moment determines the state of the cell itself and its neighbor cells (Alsamawi, 2020). Therefore, before defining the transition rule function, it is necessary to define the cellular neighbor rule [60]. The widely used neighbor types are von Neumann type, Moore type, and extended Moore type, as shown in Fig. 8. The dynamic function that determines the state of the cell at the next moment through the neighbor state and the current state is called the state evolution rule (transition function), denoted by f: $s_i^t + 1 = f(s_i^t, s_N^t)$, s_N^t is the combination of neighbor states at time t, and f is the local mapping or local rule of cellular automata. Then the dynamic evolution local function determined by the local evolution rule f of each cell is denoted by: $\mathbf{F(S_i^{t+1}) = f\,(s_{i-r}^t, \ldots, s_i^t, \ldots s_{i+r}^t).}$

3.2. Local evolution rules

CA model can be summarized as a mathematical function, expressed as $L = (L_a, S, N, \varphi)$, where.

S represents the cellular state;

L_a stands for cellular space;

a is the dimension of space;

N stands for cellular combination;

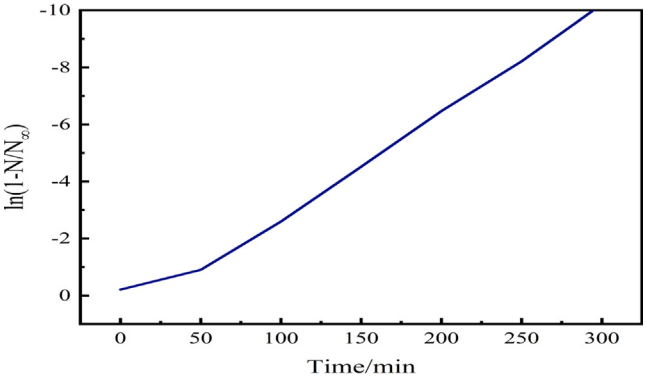

Fig. 6 Fixed temperature ln $(1\text{-}N/N_\infty)$-t curve of diffusion theory.

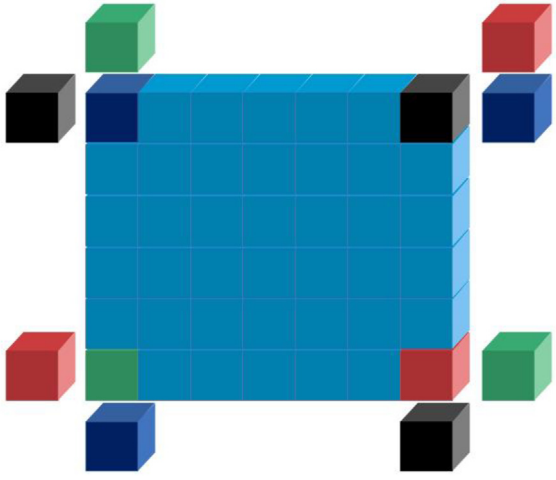

Fig. 7 Schematic diagram of top periodic boundary evolution.

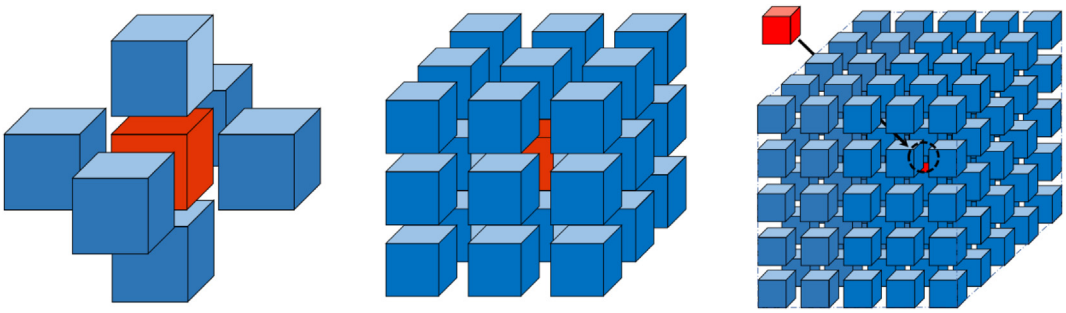

(a) Von Neumann type (b) moore model (c) Extended Moore type

Fig. 8 Cellular neighbor types.

φ represents the evolution rule of cellular state (transition function);

In this study, the three-dimensional CA model was used to simulate the corrosion pits of steel and metal in the soil corrosion environment. The metal and soil corrosion medium system was defined as a cellular grid, and $N_i \times N_j \times N_k = 100*100*100$. In order to simulate the infinity of cellular space, the von Neumann type is considered as the neighbor type, with fixed boundary conditions for upper and lower sides and periodic boundary conditions for front and back. Suppose the cell has four states, expressed as S = (M, C, N, F), Among them, M represents the metal cell that will be corroded, C represents the corrosive cell that is corrosive and can move up and down in six directions. Combined with the soil ratio scheme used in the experimental part, the corrosive cell C that can react with the metal cell M in this study includes the following ions: chloride ion, sulfate ion, bicarbonate ion, N represents the solution water molecule (the position will be occupied by the cell C at any time), F represents the passivation cell (formed by the contact of M and C). Once the passivation cell F is formed in the corrosion reaction, the state of the passivation cell will not change in the next simulation. At the same time, the cell state in the CA model can only be any of the above four. Therefore, the state of the cell at the next moment is determined by the neighbor primitives in the six directions of the cell. In addition, it is assumed that the concentration of the solution is controlled by the numerical results of C / N.

By controlling the time step of the number of iterations and the concentration of the electrolyte solution, the cell C representing the corrosive medium moves randomly in six directions: up, down, left, right, front and back. The corrosive cell C and the metal cell M react with the corrosion probability P_{cor}. The corrosion reaction between the cells is expressed by the following formula:

$$M + C + N \xrightarrow{P_{cor}} C + N \tag{22}$$

the following situations may occur in the corrosion reaction of metal cellular:

① When the dissolution reaction occurs in the contact between metal cellular M and corrosive cellular C, M dissolves with probability Pd, and the position of the original metal cellular M becomes vacant or passivated. If it is vacant, it may be occupied by water molecular cell N in the next time range. If it is a passivation state, the cell position state of the passivation cell F will not change.

② If the neighbor cell of metal cell M is corrosive cell C, and the corrosive cell C does not move in the direction of this cell M, the state of metal cell M remains unchanged.

③If the neighbor cell of metal cell M is passivation cell F or the same type of metal cell M and water molecule N, the cell state remains unchanged.

The bicarbonate ions contained in the corrosive medium in the environment will bring passivation to the metal matrix, resulting in a passivation reaction between metal cells with passivation probability Pp, expressed as:

$$M + C \xrightarrow{P_p} F + C \tag{23}$$

① If the corrosive cell C moves towards the metal cell M, the metal cell M will be dissolved by the corrosive cell C with a certain dissolution probability of Pd. In the next time step, the position of the cell M will be occupied by cell C, and the original vacancy position of the corrosive cell C will be automatically filled by the water molecule cell N, which is expressed as:

$$M + C \xrightarrow{P_d} C \tag{24}$$

② If the movement direction of the corrosive cell C is toward the same type of corrosive cell C, the original position of the corrosive cell C remains unchanged, and then a target neighbor position is randomly selected in the next time step. If the moving position in the time step of corrosive cell C is a vacant grid position, the cell may abandon the existing grid position and jump to the target position.

3.3. Analysis of effect

Considering the actual situation, and in order to have higher coincidence and consistency with the experimental results. The theoretical model sets the corrosion probability $P_{cor} = 0.89$, dissolution probability Pd = 0.8, and passivation probability Pp = 0.02. The single corrosive ion is taken as an important parameter in the CA model to optimize the model with the interaction of HCO3–, SO42- and SO42-, and the influence of the three ions on metals is taken as an important factor to set the evolution rules of the CA model. According to the soil matching scheme of the experiment, Scheme 2, in which the three ions act together, is selected as the main simulation research object of the CA model. Where, $C(HCO_3^-) = 0.192$ mol/kg, $C(SO_4^{2-}) = 0.08$ mol/kg, $C(Cl^-) = 4.24$ mol/kg,

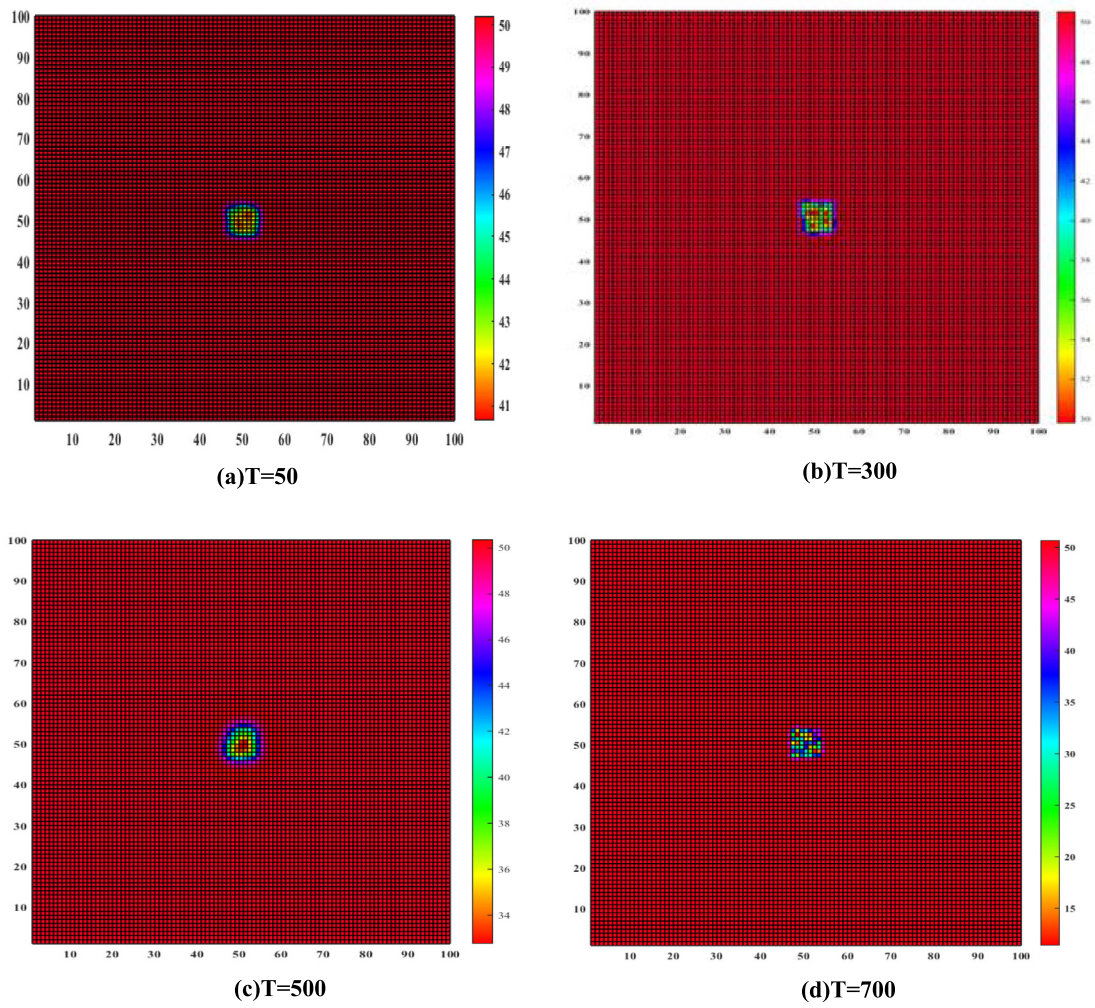

Fig. 9 Growth simulation results of initial single pit with different iteration steps.

and set the concentration of corrosion solution c = 0.2. The above ion concentration and corrosive medium concentration were substituted into the CA model for simulation. With the continuous diffusion of ions in soil towards the metal surface, the influence of chloride ions on the metal surface gradually expands with the increase of time step. At the same time, corrosion pits can randomly form on the surface of the metal that is not smooth.

Due to the unique properties of the metal itself and the influence of the corrosive medium, when the corrosion reaction occurs to produce pitting pits, the pitting pits are rarely corroded in a single pit, and most of them are accompanied by multi-pit corrosion as a common phenomenon. In this study, the formation process and results of pitting pits were idealized to some extent. The growth process of pitting pits in a certain period of time was selected as the research object, the conditions of pitting pits were limited to some extent, and it was assumed that single-pit corrosion was the main corrosion. For the case of single pit corrosion, the simulation iteration steps of the CA model were set as T = 50, T = 300, T = 500, and T = 700, respectively. According to the simulation results, it can be observed that the morphology of the corrosion pit randomly generated on the metal is an unfixed shape. As shown in Fig. 9, with the larger the time step, the corrosion pits.

Considering the early stage of corrosion behavior, localized corrosion behavior occurred on the metal surface. According to the value of the fitted corrosion rate, it was combined with the three-dimensional cellular automaton model to study the results of the three-dimensional cellular automaton model under three soil ratio schemes.

Firstly, in the soil ratio scheme 3, which is controlled by a single ion as the main influencing factor, the ion concentration of the soil ratio scheme 3 and the fitted corrosion rate value are substituted into the theoretical model of the soil ratio scheme 1, and the corrosion probability P_{cor} = 0.53 and the dissolution probability P_d = 0.8 are set. Because there is no HCO_3^- ion in the soil that causes the passivation reaction of the metal, the passivation probability P_p = 0 is considered. The individual corrosive ions are used as important parameters in the CA model. Among them, C (Cl^-) = 4.24 mol / kg, and the concentration of the corrosion solution remains unchanged. As shown in Fig. 10(a), when the iteration step size T = 700, in the case of a single high concentration of Cl^- ions used alone, with the increase of time, the three-dimensional model of the simulated metal matrix is only slightly corroded, and does

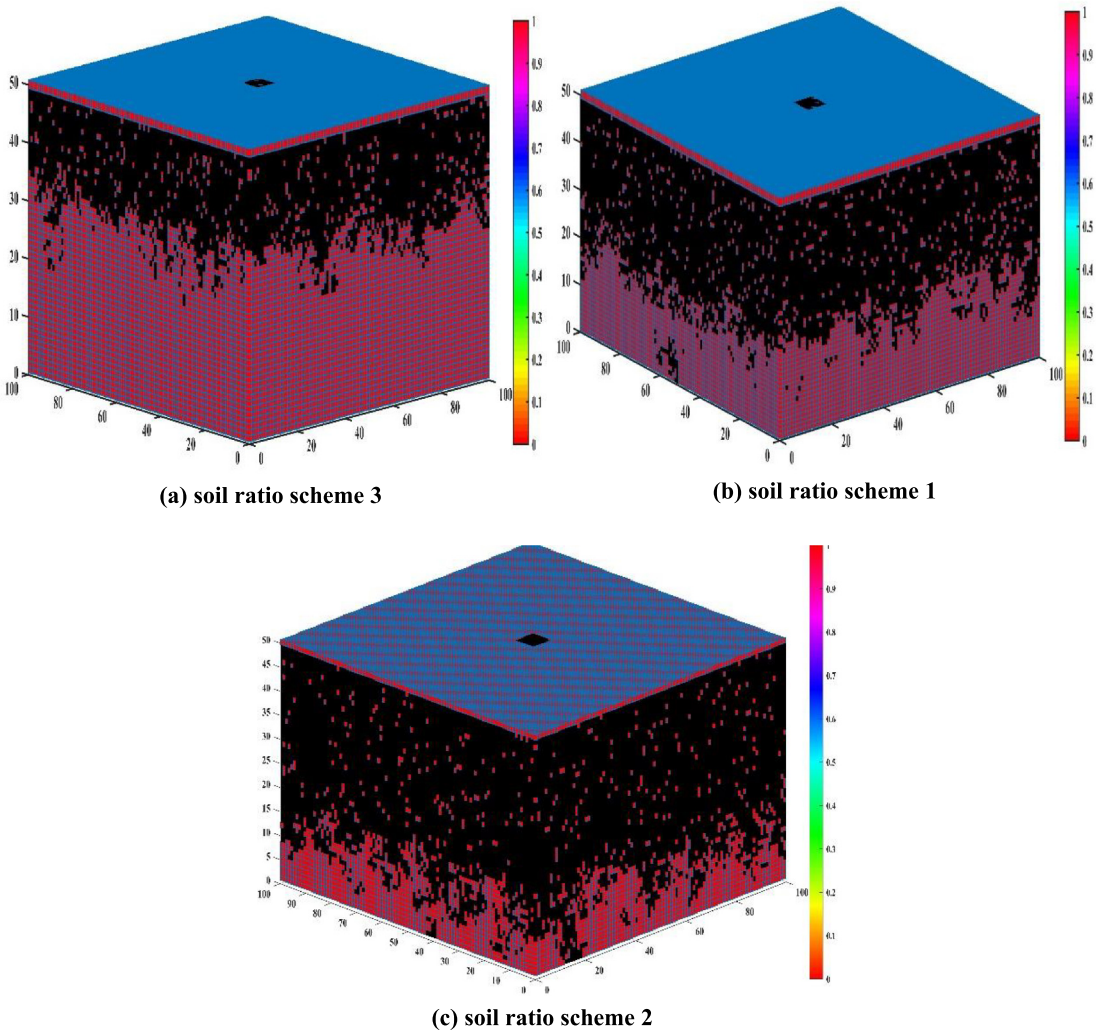

(a) soil ratio scheme 3

(b) soil ratio scheme 1

(c) soil ratio scheme 2

Fig. 10 Three-dimensional cellular machine simulation results of iterative 700-step metal corrosion under three soil ratio schemes.

not show a perforation trend. At the same time, the corrosion shown in the model is basically consistent with the law shown in the electrochemical impedance measurement and polarization curve.

Secondly, for the soil ratio scheme 1 with SO_4^{2-} and Cl^- as the influencing factors, according to the above modeling method, the ion concentration configured in the test and the approximate value of the fitted corrosion rate are substituted into the theoretical model of the soil ratio scheme 1, where the SO_4^{2-} and Cl^- concentrations are 3.16 mol / kg and 2.54 mol / kg, respectively, and the corrosion probability $P_{cor} = 0.85$ and the dissolution probability $P_d = 0.8$ are set. Similarly, there is no HCO_3^-ion in the soil ratio scheme 1, so the passivation probability $P_p = 0$ is set. As shown in Fig. 10(b), when the iteration step size T = 700, with the increase of time, the metal matrix model under the combined action of the two influencing factors has been seriously corroded and has shown a slight perforation trend. This is basically consistent with the results of experimental analysis.

Finally, Fig. 10(c) shows that in the soil ratio scheme 2, when the iteration step T = 700, taking the presence of three corrosive ions in the soil medium (where the concentrations of HCO_3^-, SO_4^{2-}, and $Cl^-$are 0.192 mol / kg, 0.08 mol/kg, and 4.24 mol/kg, respectively) as an example, under the combined action of the three ions, the model representing the simulated metal matrix has been able to exhibit severe corrosion by the corrosive medium. According to the above-mentioned hypothetical pitting single-pit corrosion phenomenon, it is assumed that the pitting behavior occurs first in the center of the matrix, and the corrosion phenomenon gradually expands from the center of the matrix to the periphery as time increases. When T = 700, according to the simulated model, it can be clearly observed that the metal matrix has shown a trend of being penetrated after being corroded by corrosive ions.

The results of the model study show that among the three soil ratio schemes, the metal matrix in scheme 3 is least affected by the corrosive medium, and the possible perforation trend on the model is also the smallest. Scheme 1 is more affected by corrosive ions than scheme 3, and has shown the possibility of perforation on the simulated metal matrix model. Scheme 3 is most affected by corrosive ions in the soil, and it has shown a penetration on the three-dimensional metal matrix model. In

summary, the corrosion behavior of the metal in the three-dimensional cellular machine is basically consistent with the results obtained from the experimental analysis.

4. Conclusion

In this study, the effect of corrosive ion diffusion in soil on the corrosion behavior of Q235 steel was studied by using the actual soil environment. The ratio of a single ion, the ratio of two ions and the ratio of three ions were considered. The metal polarization curve, open circuit potential and chemical impedance were measured by the electrochemical workstation. The Tafel law was used to fit the potential and current of the cathode and anode, and the main reasons for controlling the corrosion rate of the metal were analyzed. At the same time, the corrosion rate of the metal under the three different soil ratio schemes was compared, and the reasons for this phenomenon were analyzed.

Based on Fick two laws, the influence of the diffusion of corrosive ions in soil on the corrosion behavior of metals was studied by using the unsteady diffusion process. The potential in soil was considered in the diffusion equation, and a mathematical model for the diffusion of corrosive ions in soil was established. At the same time, combined with the three-dimensional CA model, the diffusion process of the size change of the corrosion pit on different iterative time steps T is simulated. The results show that the growth process of the corrosion pit area is consistent with the mathematical theoretical model. Combined with the fitted corrosion rate and the ion content in the soil, the three-dimensional modeling of the corrosion behavior of the metal matrix under the three soil schemes is carried out respectively. According to the analysis of the three-dimensional model, it is proved that pitting perforation may occur after the metal matrix is corroded, and the perforation behavior is directly related to the corrosion rate of the metal.

Based on the numerical and simulation results obtained from this study, the growth and expansion of corrosion pits and the process of metal corrosion damage can be further predicted, which provides a lot of useful information for studying the life integrity analysis of metal structures.

However, it is still a problem for researchers to further study the pitting effect and understand the morphology of corrosion pits. The corrosion pit caused by corrosion perforation is a cause of metal structure stability problems.

Acknowledgement

This project is supported by basic research project of provincial science and technology department (Guizhou Science and Technology Foundation ZK[2022ordinary032]).

References

Al-samawi, M., Zhu, J., 2020. Evaluation of the corrosion effects on the performance of composite bridge based on cellular automata and finite element method. Struct. Infrastruct. Eng. 18, 630–652. https://doi.org/10.1080/15732479.2020.1860095.

Apostolopoulos, C.A., Demis, S., Papadakis, V.G., 2013. Chloride-induced corrosion of steel reinforcement – Mechanical performance and pit depth analysis. Constr. Build. Mater. 38, 139–146. https://doi.org/10.1016/j.conbuildmat.2012.07.087.

Apostolopoulos, C.A., Demis, S., Papadakis, V.G., 2013. Chloride-induced corrosion of steel reinforcement – Mechanical performance and pit depth analysis. Constr. Build. Mater. 38, 139–146. https://doi.org/10.1016/j.conbuildmat.2012.07.087.

Bartosik, L., Litniewski, M., Gorecki, J., Stafiej, J., Caprio, D.D., 2014. Cellular automata based approach to corrosion and passivity related phenomena. In: International Conference on Computational Science and Computational Intelligence, pp. 272–276.

Bhandari, J., Khan, F., Abbassi, R., Garaniya, V., Ojeda, R., 2015. Modelling of pitting corrosion in marine and offshore steel structures – A technical review. J. Loss Prev. Process Ind. 37, 39–62. https://doi.org/10.1016/j.jlp.2015.06.008.

Cai, S. et al, 2022. Research on the Corrosion Behavior of Q235 Pipeline Steel in an Atmospheric Environment through Experiment. Materials 15 18. https://doi.org/10.3390/MA15186502.

Chang, C.J., Chang, C.H., Hung, T.K., 2022. A Computational pitting corrosion model of magnesium alloys. Front. Bioeng. Biotechnol. 10, 1–8. https://doi.org/10.3389/fbioe.2022.887444.

Changxu Huang, et al."Effects of temperature on acceleration and simulation of indoor corrosion test of Q235 carbon steel." Anti - Corrosion Methods and Materials 68.6(2021). doi:10.1108/ACMM-01-2021-2426.

Chen, H., Chen, Y., Zhang, J., 2008. Cellular automaton modeling on the corrosion oxidation mechanism of steel in liquid metal environment. Prog. Nucl. Energy 50, 587–593. https://doi.org/10.1016/j.pnucene.2007.11.044.

Chen, L., Wei, B., Xu, X., 2021. Effect of Sulfate-Reducing Bacteria (SRB) on the corrosion of buried pipe steel in acidic soil solution. Coatings 11, 625–639. https://doi.org/10.3390/coatings11060625.

Chen, R., Xu, Q., Liu, B., 2015. Cellular automaton simulation of three-dimensional dendrite growth in Al–7Si–Mg ternary aluminum alloys. Comput. Mater. Sci 105, 90–100. https://doi.org/10.1016/j.commatsci.2015.04.035.

Chung, N.T., So, Y.S., Kim, W.C., Kim, J.G., 2021. Evaluation of the influence of the combination of pH, chloride, and sulfate on the corrosion behavior of pipeline steel in soil using response surface methodology. Materials (Basel). 14, 1–14. https://doi.org/10.3390/ma14216596.

Cui, C., Ma, R., Chen, A., Pan, Z., Tian, H., 2019. Experimental study and 3D cellular automata simulation of corrosion pits on Q345 steel surface under salt-spray environment. Corros. Sci. 154, 80–89. https://doi.org/10.1016/j.corsci.2019.03.011.

di Caprio, D., Stafiej, J., Luciano, G., Arurault, L., 2016. 3D cellular automata simulations of intra and intergranular corrosion. Corros. Sci. 112, 438–450. https://doi.org/10.1016/j.corsci.2016.07.028.

Ezuber, H.M., Alshater, A., Hossain, S.M.Z., El-Basir, A., 2020. Impact of Soil Characteristics and Moisture Content on the Corrosion of Underground Steel Pipelines. Arab. J. Sci. Eng. 46, 6177–6188. https://doi.org/10.1007/s13369-020-04887-8.

Fatoba, O., Akid, R., 2022. The influence of corrosion pit–pit spacing on the pit-to-crack transition and fatigue lifetime. Fatigue Fract. Eng. Mater. Struct. 45, 9. https://doi.org/10.1111/FFE.13755.

Fatoba, O.O., Leiva-Garcia, R., Lishchuk, S.V., Larrosa, N.O., Akid, R., 2018. Simulation of stress-assisted localised corrosion using a cellular automaton finite element approach. Corros. Sci. 137, 83–97. https://doi.org/10.1016/j.corsci.2018.03.029.

Feng, L., He, J., Hu, L., Shi, H., Yu, C., Wang, S., et al, 2020. A parametric study on effects of pitting corrosion on steel plate's ultimate strength. Appl. Ocean Res. 95, 102026–102036. https://doi.org/10.1016/j.apor.2019.102026.

Guiso, S., Brijou-Mokrani, N., de Lamare, J., Di Caprio, D., Gwinner, B., Lorentz, V., et al, 2022. Intergranular corrosion in evolving media Experiment and modeling by cellular automata. Corros. Sci. 205, 110457–110473. https://doi.org/10.1016/j.corsci.2022.110457.

Hang, L.i., Jiahua, X., 1998. Basic equation for ion diffusion in soil together with experimental validation. J. Soil Sci. 321–327.

Hirata, R., Ooi, A., Tada, E., Nishikata, A., 2021. Influence of the degree of saturation on carbon steel corrosion in soil. Corros. Sci. 189, 109568–109668. https://doi.org/10.1016/j.corsci.2021.109568.

Jahns, K., Landwehr, M., Wübbelmann, J., Krupp, U., 2014. Numerical analysis of high temperature internal corrosion mechanisms by the cellular automata approach. Mater. Corros. 65, 305–311. https://doi.org/10.1002/maco.201307179.

Jian, M. et al, 1334. The electrochemical characteristics of corrosion scale on P110 carbon steel. Adv. Mater. Res. 1334, 287–290 www.scientific.net/AMR.287-290.2332.

Lan, Y. et al, 2021. The electrochemical corrosion behaviour of Q235 steel in soil containing sodium chloride. Int. J. Electrochem. Sci. 16 9. https://doi.org/10.20964/2021.09.31.

Law, P.E., 1985. Soil physico-chemistry, Agricultural Press.

Lei, L., Xiaogang, L., Chaofang, D., Kui, X., Lin, L., 2009. Cellular automata modeling on pitting current transients. Electrochem. Commun. 11, 1826–1829. https://doi.org/10.1016/j.elecom.2009.07.027.

Li, R., 1985. Nonequilibrium thermodynamics and dissipative structure. Tsinghua University Press.

Li, X. et al, 2021. Influence of Cl- and SO_2 on Carbon Steel Q235, Pipeline Steel L415 and Pressure Vessel Steel 16MnNi Corrosion Behavior in Industrial and Marine Atmosphere Environment. Int. J. Electrochem. Sci. 16 11. https://doi.org/10.20964/2021.12.06.

Liu, M. et al, 2022. Synergistic Effect of Different NaCl concentrations on the initial corrosion of Q235 Steel under a simulated SO_2 environment. ChemistrySelect 7 7. https://doi.org/10.1002/SLCT.202103257.

Liu, H., Dai, Y., Cheng, Y.F., 2020. Corrosion of underground pipelines in clay soil with varied soil layer thicknesses and aerations. Arab. J. Chem. 13, 3601–3614. https://doi.org/10.1016/j.arabjc.2019.11.006.

Long, J.-Y., Zhao, T.-T., Yuan, M.-Y., Yang, Y.-T., 2020. Experimental study and cellular automata simulation of corrosion behavior of ferritic stainless steel in molten aluminum. J. Iron Steel Res. Int. 29 (9), 1485–1494. https://doi.org/10.1007/s42243-022-00807-2.

Pérez-Brokate, C.F., di Caprio, D., Féron, D., de Lamare, J., Chaussé, A., 2016. Three-dimensional discrete stochastic model of occluded corrosion cell. Corros. Sci. 111, 230–241. https://doi.org/10.1016/j.corsci.2016.04.009.

Pérez-Brokate, C.F., di Caprio, D., Féron, D., de Lamare, J., Chaussé, A., 2017. Pitting corrosion modelling by means of a stochastic cellular automata-based model. Corros. Eng. Sci. Technol. 52, 605–610. https://doi.org/10.1080/1478422x.2017.1311074.

Pidaparti, R.M., Rao, A.S., 2008. Analysis of pits induced stresses due to metal corrosion. Corros. Sci. 50, 1932–1938. https://doi.org/10.1016/j.corsci.05.003.

Puspalata, R. et al, 2022. Chemistry conditions and corrosion behaviour in simulated crevices of alloy steel. Corros. Eng. Sci. Technol. 57 4. https://doi.org/10.1080/1478422X.2022.2063780.

Qi, G. et al, 2022. Electrochemical corrosion behaviour of four low-carbon steels in saline soil. RSC Adv. 12 32. https://doi.org/10.1039/D2RA03200G.

Qi, G., Qin, X., Xie, J., Han, P., He, B., 2022. Electrochemical corrosion behaviour of four low-carbon steels in saline soil. RSC Adv. 12, 20929–20945. https://doi.org/10.1039/d2ra03200g.

Quan, B., Li, J., Chen, C., 2021. Effect of Corrosion time on the synergistic corrosion of Q235 steel in sodium aluminate solutions.". Metals 11 5. https://doi.org/10.3390/MET11050753.

Rusyn, B.P., Tors'ka, R.V., Pokhmurs'kyi, A.Y., 2015. Modeling of the evolution of corrosion pitting with the use of cellular automata. Mater. Sci. 50, 706–713. https://doi.org/10.1007/s11003-015-9775-2.

Rybalka, K.V., Shaldaev, V.S., Beketaeva, L.A., Malofeeva, A.N., Davydov, A.D., 2010. Development of pitting corrosion of stainless steel 403 in sodium chloride solutions. Russ. J. Electrochem. 46, 196–204.

Safira, F. et al, 2018. Corrosion behaviour of carbon steel in aqueous solution containing Galena concentrate. IOP Conference Series: Materials Science and Engineering 352 1. https://doi.org/10.1088/1757-899X/352/1/012001.

Saunier, J., Chaussé, A., Stafiej, J., Badiali, J.P., 2004. Simulations of diffusion limited corrosion at the metal|environment interface. J. Electroanal. Chem. 563, 239–247. https://doi.org/10.1016/j.jelechem.2003.09.017.

Saunier, J., Dymitrowska, M., Chaussé, A., Stafiej, J., Badiali, J.P., 2006. Diffusion, interactions and universal behavior in a corrosion growth model. J. Electroanal. Chem. 582, 267–273. https://doi.org/10.1016/j.jelechem.2005.03.047.

Stępień, J., Stafiej, J., 2018. Potential oscillations in cellular automaton based model for passivation of metal surface, developments in language theory. 92-101. https://doi.org/10.1007/978-3-319-99813-8_892-101.

Valor, A., Caleyo, F., Alfonso, L., Rivas, D., Hallen, J.M., 2007. Stochastic modeling of pitting corrosion A new model for initiation and growth of multiple corrosion pits. Corros. Sci. 49, 559–579. https://doi.org/10.1016/j.corsci.2006.05.049.

Wang, R., 2021. On the effect of pit shape on pitted plates, Part II Compressive behavior due to random pitting corrosion. Ocean Eng. 236, 108737–108756. https://doi.org/10.1016/j.oceaneng.2021.108737.

Wang, C. et al, 2022. Corrosion behavior of Q235 steel by synergistic action of high concentration Cl− and complex scale in mixed salt flooding. Vacuum 204. https://doi.org/10.1016/J.VACUUM.2022.111365.

Wang, H. T. and E. H. Han, Cellular automata simulation of interactions between metastable corrosion pits on stainless steel, Materials and Corrosion. 66(2015) 925-930.https://doi.org/10.1002/maco.201408057.

Wang, W., Guan, B., Wei, X., Lu, J., Ding, J., 2019. Cellular automata simulation on the corrosion behavior of Ni-base alloy in chloride molten salt. Sol. Energy Mater. Sol. Cells 203, 110170–110180. https://doi.org/10.1016/j.solmat.2019.110170.

Wang, H., Han, E.-H., 2016. Computational simulation of corrosion pit interactions under mechanochemical effects using a cellular automaton/finite element model. Corros. Sci. 103, 305–311. https://doi.org/10.1016/j.corsci.2015.11.034.

Wang, X., Wang, J., Zhou, X., Xie, Y., Chen, J., Ding, Z., Wu, T., Luo, J., Yin, F., 2022. Short-Term corrosion characteristic of Q235 steel under different atmospheric environments of Hunan. J. Mater. Eng. Perform. 31 (10). https://doi.org/10.1007/S11665-022-06839-9.

Wang, B., Zhang, T., Liu, Y., Cui, G., 2021. Corrosion Damage Behavior of X65 Incoloy 825 Welded Bimetallic Composite Pipe in H2S Environment. Front. Mater. 8, 1–12. https://doi.org/10.3389/fmats.2021.709101.

Wei, B., Qin, Q., Fu, Q., Bai, Y., Xu, J., Yu, C., et al, 2020. X80 Steel Corrosion Induced by Alternating Current in Water-Saturated Acidic Soil. Corrosion 76, 248–267. https://doi.org/10.5006/3418.

Xu, Z., Lu, J., Wei, X., Ding, J., Wang, W., 2022. 2D and 3D cellular automata simulation on the corrosion behaviour of Ni-based alloy in ternary molten salt of NaCl–KCl–$ZnCl_2$. Sol. Energy Mater. Sol. Cells 240, 111694–111706. https://doi.org/10.1016/j.solmat.2022.111694.

Xuefeng, L., H. Lei and C. Dongmei, Simulation of pit interactions of multi-pit corrosion under an anticorrosive coating with a three-dimensional cellular automata model, Modelling and Simulation in Materials Science and Engineering. 29(2021) 65018-65045. https //doi.org/ 10.1088/1361-651X/ac13cb.

Zenkri, M., di Caprio, D., Raouafi, F., Féron, D., 2022. Cathodic control using cellular automata approach. Mater. Corros. 73, 1631–1643. https://doi.org/10.1002/maco.202213054.

Zhang, X., Zhao, J., Jiang, H., Zhu, M., 2012. A three-dimensional cellular automaton model for dendritic growth in multi-component alloys. Acta Mater. 60, 2249–2257. https://doi.org/10.1016/j.actamat.2011.12.045.

Zhou, X. et al, 2022. Study on corrosion behavior of Q235 steel in a simulated marine tidal environment. J. Mater. Eng. Perform. https://doi.org/10.1007/S11665-021-06551-0.